2022 IEEE International Conference on Environment and Electrical Engineering and 2022 IEEE Industrial and Commercial Power Systems Europe (EEEIC / I&CPS Europe) | 978-1-6654-8537-1/22/$31.00 ©2022 IEEE | DOI: 10.1109/EEEIC/ICPSEUROPE54979.2022.9854580

Low concentration photovoltaic systems based on small-scale linear Fresnel reflectors: Development of a new sawtooth V-trough concentrator

José Ángel Fernández Rubiera
Department of Electric Engineering
University of Oviedo
Gijón, Spain
fernandezrjose@uniovi.es

Arsenio Barbón
Department of Electric Engineering
University of Oviedo
Gijón, Spain
barbon@uniovi.es

Luis Bayón
Department of Mathematics
University of Oviedo
Gijón, Spain
bayon@uniovi.es

Guzmán Díaz
Department of Electric Engineering
University of Oviedo
Gijón, Spain
guzman@uniovi.es

Covadonga Bayón-Cueli
Polytechnic School of Engineering
University of Oviedo
Gijón, Spain
cobayon18@gmail.com

***Abstract*—This study focuses on the design of the receiver cavity of a small-scale linear Fresnel reflector used as sunlight collector in a lowconcentration photovoltaic system. Since photovoltaic cells require uniform illumination over their entire surface for their correct operation, this will be the key point of the design. This work aims to investigate the geometry of a new sawtooth Vtrough cavity. The design is first carried out from a theoretical point of view, obtaining the general equations. These equations will be verified using the Monte Carlo Ray Tracing method. The SolTrace™ software will be used for this purpose.**

***Index Terms*—Low-concentration Photovoltaic systems, Linear Fresnel reflector, Sawtooth V-trough cavity, SolTrace™ software.**

I. Introduction

In recent years, non-concentrated photovoltaic (PV) systems have been seen as key technologies in the fight against climate change. This is due to, among other factors: the characteristics of its components allow freedom of installation, the commercial availability, and the decrease in its levelised cost of energy ($LCoE$). However, this technology only converts 15-18% of the incident solar irradiance into electricity, while the remaining is converted into thermal energy [1]. Therefore, a large area of photovoltaic cells is required. These characteristics limit their applications.

Concentrated photovoltaic (CPV) systems concentrates solar irradiance onto a small area of the photovoltaic cell with the help of lenses and optics. Therefore, these systems reduce the area of photovoltaic cells. In addition, they improves conversion efficiency performance.

A number of studies have been published on CPV systems using several types of sunlight collectors: parabolic dish [2], parabolic trough [3], central receiver [4], Fresnel lenses [5] and small-scale linear Fresnel reflector [6]. CPV systems can be classified according to the concentration level such as low $(2-10$ suns), medium $(10-100$ suns) and high $(100-2000$ suns) concentration systems [1].

On the other hand, the energy needs of the building sector comprise electrical and thermal energy. Therefore, low-concentration photovoltaic ($LCPV$) systems can be the solution to cover these energy needs.

This study focuses on the design of the receiver cavity of a small-scale linear Fresnel reflector ($SSLFR$) used as sunlight collector in a $LCPV$. This $SSLFR$ uses rows of mirrors to focus the incident solar irradiance onto a set of PV cells running longitudinally above the rows of mirrors and is located on the common focal line of the mirrors.

The efficiency of $LCPV$ depends to a large extent on the efficiency of the photovoltaic cells, which require uniform illumination over their entire surface for their correct operation.

Non-uniform illumination causes serious problems in the operation of the PV cells such as: (i) higher than expected ohmic drops [7]; (ii) mismatches between photovoltaic cells connected in series [8], and (iii) hotspots [8].

Rabl [9] states the fundamental problem in the design of concentrators by means of the area or geometric concentration ratio:

$$C_a = \frac{\text{aperture area}}{\text{absorber area}} = \frac{A_a}{A_{abs}} \quad (1)$$

From the Second Law of Thermodynamics, Rabl [9] concludes that the maximum possible geometric concentration ratio for a given acceptance half angle θ_c is: $C_{ideal}^{2D} = \sin^{-1}\theta_c$. There are other indices in the literature which measure the goodness of a concentrator:

978-1-6654-8537-1/22/$31.00 ©2022 IEEE

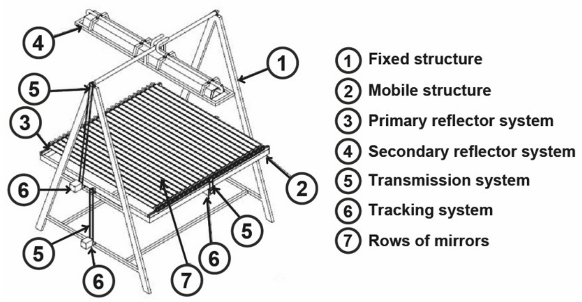

Fig. 1. Scheme of $SSLFR$.

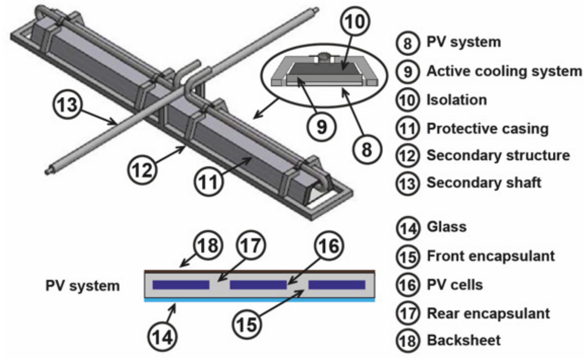

Fig. 2. Secondary reflector system.

the flux concentration ratio [10]:

$$C_{opt} = \frac{\text{flux at the receiver}}{\text{flux at the absorber}} = C_a \cdot \eta_{ray} \tag{2}$$

where C_{opt} is the optical concentration ratio, C_a is the area concentration ratio, and η_{ray} is the ray acceptance rate. η_{ray} gives the fraction of incident light rays reaching the absorber.

Finally, in order to carry out a cost analysis, another parameter is needed: the reflector-to-aperture area ratio (in which the height plays clearly a role):

$$R_a = \frac{\text{reflector area}}{\text{aperture area}} = \frac{A_r}{A_a} \tag{3}$$

Consequently, this work aims to investigate the geometry of a sawtooth V-trough cavity such as the height of the cavity (H), the trough wall angle (WA) (τ), and the base opening (B).

II. Brief description of the SSLFR

The system is composed of two main parts: the primary reflector system and the secondary system. The component elements are specified in Figs. 1 and 2. The primary reflector system contains the parallel mirror rows and the various tracking elements. The primary reflector system is mounted on a mobile structure, as shown in Fig. 1.

The secondary system (see Fig. 2) is mounted on a fixed structure, located at a specific height above the primary reflector system, and is composed of the secondary structure and shaft (needed for proper placement), the PV system, the active cooling system, the isolation material, and a protective casing. The cells are the smallest unit of the PV system, there being several of them interconnected and encapsulated. Most of the solar irradiance absorbed by the PV cells is converted into heat, so that a cooling system is required (otherwise they either malfunction or work inefficiently).

Its main constructive magnitudes are: width of the i-th mirror (W_{Mi}), height to the receiver (f), separation between two consecutive mirrors (d_i), distance from the mirror centers to the center of $SSLFR$ (L_i), width of the PV cells (b), aperture of the V-trough cavity (B), number of V-trough cavities of the sawtooth (m) and number of mirrors on each side of the SSLFR ($N_r = N_l$, which we shall call N, as we assume the same number of mirrors on each side). The secondary cavity is symmetric with respect to the central axis.

III. Design of a sawtooth V-trough

In this section we provide a detailed description of the optimal design of the sawtooth V-trough cavity, using analytical formulas exclusively. The sawtooth V-trough cavity consists of a number of V-trough cavities as shown in Fig. 3.

Consider a classical single-focus V-cavity (Vtrough cavity m) as shown on Fig. 3. There are two linear, slanted sides (PQ and $P'Q'$) which concentrate light from the wider inlet opening PP' towards the narrower absorber area QQ'. We are going to consider four parameters: inlet radiation, the trough wall angle (WA) τ, the height H and the base opening B. The upper width QQ' is not a free parameter but a constraint, because it equals the width of the PV cells. Notice that our angle τ is the complement of Hollands [11] and Rabl's [9] Φ. Moreover, the key point of our design is to achieve uniform illumination of the PV cells, therefore, we aim for a 100% of incoming radiation reaching the PV cells, that is, given an acceptance angle θ_c, the ray acceptance rate η_{ray} must be 1, from which follows:

$$C_{opt} = C_a; \ |\theta_i| \leq |\theta_c| \tag{4}$$

Where θ_i is the incidence angle of each ray. The central axis OR will be the reference axis for angles, and we shall consider θ_i to be positive for rays coming from the left side, and negative for those coming from the right.

For simplicity, we shall denote the angle between the ray reaching the cavity and OR as α_0 (i.e. $\alpha_0 = \theta_i$), and each of its successive reflections will be α_j, for $j = 1, 2, \ldots$. In these terms, the problem can be stated as: given b, in order to find the maximum C_a, we shall maximize B under the restriction that all the rays reaching PP', after a number of reflections, get to the PV cell (whose width is b), that is $\eta_{ray} = 1$:

$$\max C_a = \max B; \ |\theta_i| \leq |\theta_c| \tag{5}$$

There are exactly two (symmetric) worst-case scenarios, of which we shall describe only one, for brevity: when the ray coming from the left side is reflected on P', with $\theta_i = \theta_c$. Using the notation of Fig. 3:

$$\theta_i = \alpha_0 \tag{6}$$

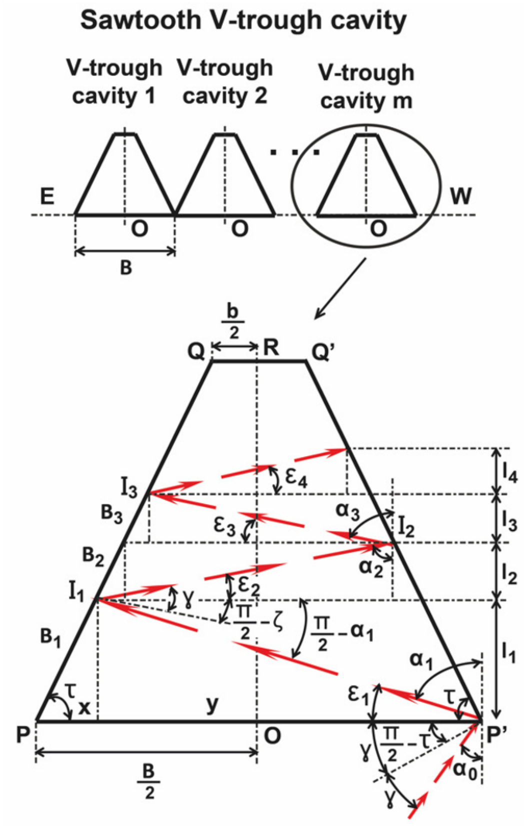

Fig. 3. Sketch of the sawtooth V-trough cavity.

Using the Law of Reflection, if n is the number of reflections required to reach the PV cells, the following equalities follow:

$$\alpha_1 = (\pi - 2\tau) + \alpha_0; \tag{7}$$
$$\alpha_2 = (\pi - 2\tau) + \alpha_1; \ \cdots \tag{8}$$
$$\alpha_n = (\pi - 2\tau) + \alpha_{n-1} \tag{9}$$

Or, just as a function of α_0:

$$\alpha_n = n(\pi - 2\tau) + \alpha_0 \tag{10}$$

As for the angle between PP' and the $i-$th reflection, called ε_j:

$$\varepsilon_1 = (2\tau - \pi/2) - \alpha_0; \tag{11}$$
$$\varepsilon_2 = (2\tau - \pi/2) - \alpha_1; \ \cdots \tag{12}$$
$$\varepsilon_n = (2\tau - \pi/2) - \alpha_{n-1} \tag{13}$$

And furthermore:

$$\varepsilon_n = \frac{\pi}{2} - \alpha_n \Rightarrow \tan\alpha_n = \cot\varepsilon_n \tag{14}$$

Finally, the vertical lengths traveled by the reflected ray l_i after each reflection are given by:

$$l_1 = \frac{B}{\cot\tau + \tan\alpha_1}; \ l_2 = \frac{B - 2(l_1)\cot\tau}{\cot\tau + \tan\alpha_2}; \tag{15}$$
$$l_3 = \frac{B - 2(l_1 + l_2)\cot\tau}{\cot\tau + \tan\alpha_3}; \ \cdots \tag{16}$$
$$l_n = \frac{B - 2\sum_{i=1}^{n-1}(l_i)\cot\tau}{\cot\tau + \tan\alpha_n} \tag{17}$$

We now have the tools required for describing the algorithm which gives the optimal design (5). The nested structure of the formulas leads to an easily implementable method.

The following property is key to finding the optimal design.

Property 1. In order to achieve (5), the optimal solution of the most unfavorable case is that in which the vertical component of each reflection on the walls (if there are any) is largest and touches the base b either on Q or Q'.

Using Property 1, we start the iterative algorithm stating a sequence of different cases C_n, for an increasing number of reflections n. We shall use, in each of them, the worst-case condition $\theta_i = \theta_c$. For each case C_n, the height of the cavity H_n (which turns out to be a function of B) can be computed using (15):

$$H_n(B) = \sum_{i=1}^{n} l_i \tag{18}$$

Now we substitute the value of $H_n(B)$ into the formula relating b, B and H with τ:

$$B = b + 2H_n(B)\cot\tau \tag{19}$$

and, solving for B, after some easy computations, we obtain:

$$\begin{aligned}
&(C_1)\ B_1(\tau) = -b\cos(\alpha_0 - 3\tau)\sec(\alpha_0 - \tau);\\
&(C_2)\ B_2(\tau) = b\cos(\alpha_0 - 5\tau)\sec(\alpha_0 - \tau);\\
&(C_3)\ B_3(\tau) = -b\cos(\alpha_0 - 7\tau)\sec(\alpha_0 - \tau);\ \ldots\\
&(C_n)\ B_n(\tau) = (-1)^n b\cos(\alpha_0 - (2n+1)\tau)\sec(\alpha_0 - \tau)
\end{aligned} \tag{20}$$

This gives the functions $B_n(\tau)$ analytically in terms of b and α_0. In the last step of the algorithm, we need to compute the maximum of those $B_n(\tau)$ in order to obtain the optimum angles τ_n^* maximizing B, and hence C_a.

The process can be made as long as desired, and we can choose the optimal design depending on the number of reflections n. From the qualitative point of view, the main result is that, the larger n, the larger B_n, so that C_a increases as well. Actually, C_a tends asymptotically to the ideal value. In each case C_n, the number of reflections is n.

Finally, in order to compute the approximate value of n we shall use the property proved by Rabl [9] that the average number of reflections in a V-trough is essentially the same as those in a compound parabolic concentrators (CPC). Thus, we consider a truncated CPC with the same height as our one-focus V-trough, starting with a whole CPC designed for the specific value of θ_c. We must not forget that the influence of n on the factor ρ_m^n is rather small because ρ_m is always very near to 1.

Having theoretically analysed a single V-trough cavity (V-trough cavity m), the proposed design consists of placing several cavities as shown in Fig.3. This design maintains the optical properties of the V-trough cavity m, but has some advantages: lower height of the cavity, more compact design, easier installation and better efficiency of the cooling system, and easier electrical connections.

IV. Uniform illumination of the PV cells

In an SSLFR the rows of mirrors can be rotated on the North-South axis so as to follow the Sun's daily movement. The mirrors move synchronously with the transversal angle θ_t:

$$\theta_t = \arctan\left(\frac{\sin\gamma_S}{\tan\alpha_S}\right) \tag{21}$$

where α_S is the solar altitude and γ_S is the solar azimuth, both of which depend on the declination δ, latitude λ and hour angle ω *[12]*. For each location, θ_t depends only on the day of the year N_d and the solar time T:

$$\theta_t = F(N_d, T) \Rightarrow T = h(N_d, \theta_t) \tag{22}$$

We shall call θ_{t_0} the worst time of the day, and we shall call the "worst mirror", the one farthest from the Sun at t_0. In the paper [6] the authors calculated the distance between mirrors which guarantees the absence of shading and blocking between two consecutive mirrors, during the operation interval (in transversal angles):

$$\theta_t \in [-\theta_{t_0}, \theta_{t_0}] \tag{23}$$

We can now define the optimum operating interval as a function of T:

$$T \in I_{N_d} = [h_R(N_d, \theta_{t_0}), h_S(N_d, \theta_{t_0})] \tag{24}$$

While in [6] the design focused on the primary reflector system, considering a single PV cell, in the present work we focus on the design of the secondary system. To link the two studies we simply consider that the focus to which all the mirrors of the primary field will point will be the geometrical centre of the sawtooth V-trough cavity.

Finally, it should be noted that the power reaching the PV cells can be calculated using the following formula proposed by [6]:

$$Q = \sum_{i=1}^{2\cdot N+1} DNI \cdot \eta_{opt} \cdot L_{PV} \cdot W_{PV} \cdot F_{bs} \cdot \cos\theta_i \cdot \cos\theta_l \tag{25}$$

where DNI is the direct normal irradiance (W/m^2), η_{opt} the optical efficiency of the $SSLFR$, the effectively illuminated length is L_{PV}. In addition, during the optimum operation time I_{N_d}, all the width of the PV cell W_{PV} is illuminated. A shading and blocking factor F_{bs} must be included, whose value is 1 during the operating interval I_{N_d} (there is none of either). The transverse angle θ_i between the normal to the i-th mirror and the incidence angle of the Sun is:

$$\cos\theta_i = \cos(\beta_i \pm \alpha_i) \tag{26}$$

and with the configuration chosen in the longitudinal study:

$$\theta_l = \theta_z/2 \tag{27}$$

Where θ_t is the longitudinal angle and θ_z is the zenith angle.

With all this, we are going to calculate the sum of the power Q of all mirrors, for all hours in working interval I_{N_d} and all days of the year N_d:

$$\sum_{N_d=1}^{365} \int_{h_R(N_d,\theta_{t_0})}^{h_S(N_d,\theta_{t_0})} Q \cdot dT \tag{28}$$

In that interval, we know for sure that there is neither shading nor blocking and the illumination is uniform.

V. Numerical results and verification

In this section we present the results obtained at a location in Almería (Spain), whose geographical data are: latitude $36°50'07''N$, longitude $02°24'08''W$ and elevation 22 m. Consider a design with: sawtooth V-trough cavity width equal to 0.20 m, $n = 3$ (i.e. 7 mirrors in total), and $f = 1.5$ m. With these starting values, an adequately dimensioned $SSLFR$ is obtained. In addition, $\theta_{t_0} = 50\ ^o$ is used. All the computations have been carried out on a budget PC using the Mathematica™ Computer Algebra System. Table I contains the geometric values of L_i and W_M for this optimal design. At this point, we number the mirrors from left to right starting at 1. As there are 7 mirrors, the central one is number 4.

Table I. Geometric values of the optimal design.

Mirror	L_i [cm]	W_M [cm]
1	101.02	22.3152
2	66.4932	22.8802
3	32.3561	22.8288
4	0	22.0676
5	32.3561	22.8288
6	66.4932	22.8802
7	101.02	22.3152

In Table II we include the fixed parameters of the $SSLFR$ considered for simulation and verification.

Table II. Fixed Parameters of the SSLFR.

	Parameters	Value
L_{PV}	PV system length	2.00 m
f	Height of the receiver	1.50 m
L_M	Mirror length	2.00 m
ρ	Mirror reflectivity	0.94
CI_m	Mirror cleanliness	0.96
CI_g	Glass cleanliness	0.96
τ_g	Glass transmissivity	0.92

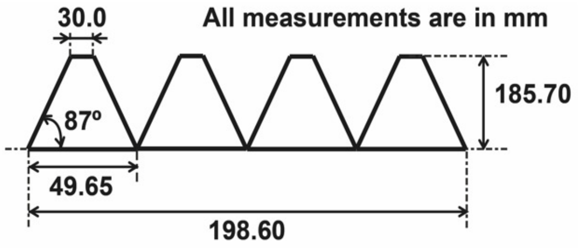

Fig. 4. Final design of the sawtooth V-trough cavity.

Table III summarize the results for $b = 30$ mm and $\theta_c = 34$ ^{o}. The annual energy is equal to 2.38266 MWh.

Table III. Results of the study.

	Parameters	Value
C_a	Area concentration ratio	1.655
τ^*	Trough wall angle	87.00 ^{o}
B	Aperture of the V-trough cavity	49.65 mm
H	Height of the V-trough cavity	185.70 m
m	Number of V-trough cavities	4

Figure 4 shows the final design of the sawtooth V-trough cavity.

A. Verification by Monte Carlo simulation

The calculations performed will be verified using the Monte Carlo Ray Tracing method. The SolTrace™ software will be used for this purpose. Based on the results obtained with the above method, a 3D model of the optimal $SSLFR$ design has been developed. Some assumptions have to be taken into account: (i) All the mirrors are flat and perfect; (ii) The rows of mirrors are perfectly tracked so as to follow the apparent movement of the Sun; and (iii) The parameters of the $SSLFR$ listed in Table II, remain constant in this study. We choose 10^7 rays for the simulation and the direct normal irradiance for each day of the year follows [13].

We show two moments. The first, inside the optimum operation interval ($T = 9.00$ hours). And the second, outside the optimum operation interval ($T = 7.00$ hours).

Figs. 5 and 6 correspond to times inside the optimum operation interval. Fig. 5 shows a snapshot of the output of SolTrace for $N = 172$, $T = 9.00$ hours. The flux density on the PV cells for $N = 172$, $T = 9.00$ hours obtained with SolTrace is provided in Fig. 6. The flux density is totally homogeneous on the PV cells. Figs. 7 and 8 correspond to times outside the optimum operation interval. Fig. 7 shows a snapshot of the output of SolTrace for $N = 172$, $T = 7.00$ hours. The flux density on the PV cells for $N = 172$, $T = 7.00$ hours obtained with SolTrace is provided in Fig. 8. The flux density is not homogeneous in photovoltaic cells.

VI. Conclusions

The design of the secondary cavity of a small-scale linear Fresnel reflector is key to maximizing the concentration ratio, which allows for a decrease in the number of photovoltaic cells required and for an increase in the width of the mirrors of the primary field, both of which lower the final cost. In this work, we have computed, analytically, the optimal design of a sawtooth V-trough cavity which, using an uniform distribution of the irradiance reaching its opening. Our analytic approach provides equations for any number of reflections, which are easily implemented as an iterative algorithm. These equations will be verified using the Monte Carlo Ray Tracing method. The SolTrace™ software will be used for this purpose. This design has some advantages: lower height of the cavity, more compact design, easier installation and better efficiency of the

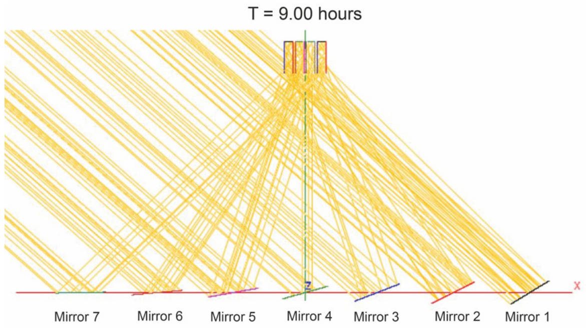

Fig. 5. A SolTrace 2D view of SSLFR for $N = 172$, $T = 9.00$ (hours).

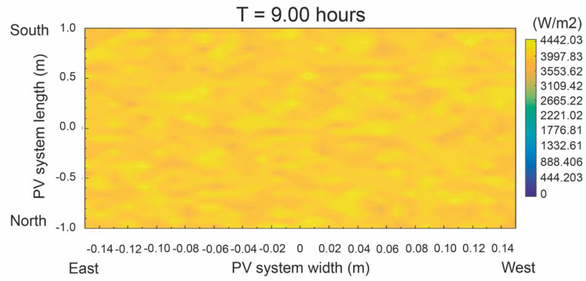

Fig. 6. SolTrace 2D view of flux density in PV cells for $N = 172$, $T = 9.00$ $(hours)$.

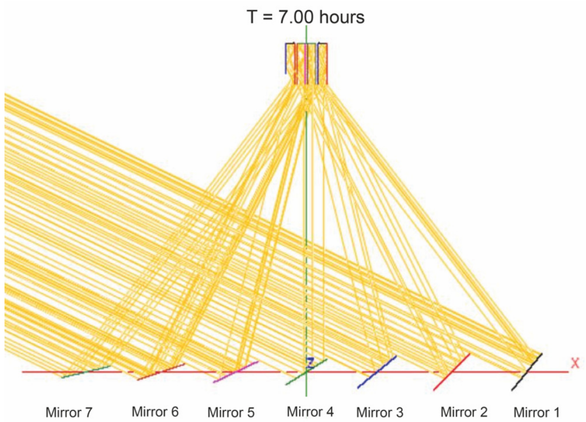

Fig. 7. A SolTrace 2D view of SSLFR for $N = 172$, $T = 7.00$ (hours).

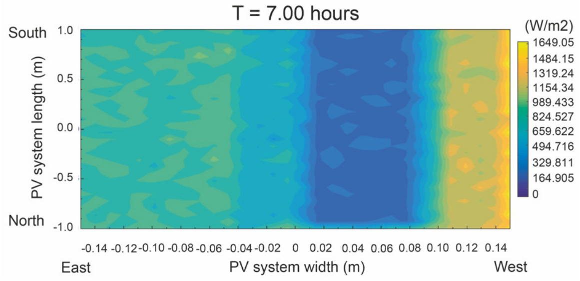

Fig. 8. SolTrace 2D view of flux density in PV cells for $N = 172, T = 7.00$ $(hours)$.

cooling system, and easier electrical connections.

References

[1] A. Ejaz, H. Babar, H.M. Ali, F. Jamil, M.M. Janjua, I.M. Rizwanul Fattah, Z. Said, C. Li, Concentrated photovoltaics as light harvesters: Outlook, recent progress, and challenges, Sustainable Energy Technologies and Assessments 46 (2021) 101199.

[2] S. Lokeswaran, T.K. Mallick, K.S. Reddy, Design and analysis of dense array CPV receiver for square parabolic dish system with CPC array as secondary concentrator, Solar Energy 199 (2020) 782–795.

[3] X. Ju, C. Xu, X. Han, X. Du, G. Wei, Y. Yang, A review of the concentrated photovoltaic/thermal (CPVT) hybrid solar systems based on the spectral beam splitting technology, Applied Energy 187 (2017) 534–563.

[4] H. Helmers, W.Y. Thor, T. Schmidt, D.W. van Rooyen, A.W. Bett, Optical analysis of deviations in a concentrating photovoltaics central receiver system with a flux homogenizer, Applied Optics 52 (2013) 2974-2984.

[5] S. Cucco, R. Faranda, F. Invernizzi, S. Leva, Analysis of a Fresnel lenses concentrator, In: 2012 IEEE Power and Energy Society General Meeting, 2012.

[6] A. Barbón, P. Fortuny Ayuso, L. Bayón, J.A. Fernández-Rubiera, Non-uniform illumination in low concentration photovoltaic systems based on small-scale linear Fresnel reflectors, Energy 239 (2022) 122217.

[7] H. Baig, K.C. Heasman, T.K. Mallick, Non-uniform illumination in concentrating solar cells, Renewable Sustain Energy Reviews 16 (2012) 5890–5909.

[8] A.B. Or, J. Appelbaum, Performance analysis of concentrator photovoltaic dense-arrays under non-uniform irradiance, Solar Energy Materials & Solar Cells 117 (2013) 110–119.

[9] A. Rabl, Comparison of solar concentrators, Solar energy 18 (1976) 93-111.

[10] H. Hadavinia, S. Harjit, Modelling and experimental analysis of low concentrating solar panels for use in building integrated and applied photovoltaic (BIPV/BAPV) systems, Renewable energy 139 (2019) 815-829.

[11] K.G.T. Hollands, A concentrator for thin-film solar cells, Solar Energy 13 (1971), 149-163.

[12] Duffie JA, Beckman WA. Solar Engineering of Thermal Processes. John Wiley & Sons; 2013.

[13] A. Barbón, P. Fortuny Ayuso, L. Bayón, J.A. Fernández-Rubiera, Predicting beam and diffuse horizontal irradiance using Fourier expansions, Renewable Energy 154 (2020) 46-57.